

Robust Control of Induction motor using Fuzzy Sliding Adaptive Controller with Sliding Mode Torque Observer

*Byung-Do Yoon **Hong-Woo Rhew **Ick-Hun Lim **Chan-Ki Kim

*Dept. of Electrical Eng., Chung-Ang Univ.,
221, Huksuk-Dong, Seoul, Korea.

**Korea Electric Power Research Institute.,
Munji-Dong, Yuseong-Gu, Taejeon, Korea.

Abstract - In this paper a robust speed controller for an induction motor is proposed. The speed controller consists of a fuzzy sliding adaptive controller(FSAC) and a sliding mode torque observer(SMTO). FSAC removes the problem of oscillations caused by discontinuous inputs of the sliding mode controller. The controller also provides robust characteristics against parameter and sampling time variations. Although, however, the performance of FSAC is better than PI controller and fuzzy controller in robustness, it generates the problem of slow response time. To alleviate this problem, a compensator, which performs feedforward control using torque signals produced by SMTO, is added.

The simulation and hardware implementation results show that the proposed system is robust to the load disturbance, parameter variations, and measurement noises.

I. INTRODUCTION

A high performance motor drive system must have a good speed command tracking and load regulating responses, and the system should be insensitive to the characteristics of the drive system. The uncertainties usually are composed of plant variations, external load disturbance, and nonlinear dynamics of the plant. Many researches on servo control have been reported for the robust speed control of an induction motor [1]. However, it is difficult to obtain a desirable servo characteristics because of an uncertain measurement of system parameter or unknown disturbance. Furthermore it requires a lot of computation to realize such sophisticated control algorithms [2]. It may also raise the stability problem in whole system due to increase of sampling time. One of control algorithm to solve this problem is the sliding mode control. The sliding mode control yields robust control for load disturbance and accurate tracking control. However, the main drawback of the sliding mode control is chattering due to discontinuous input. Although several methods to remove this chattering have been reported[1],[2],[3], they are very complicated to actually implement. Furthermore, they reduce robustness.

In this paper a robust speed controller for an induction motor is proposed. The speed controller consists of a FSAC and SMTO. Although the performance of (FSAC) is better than PI controller and fuzzy controller in robustness, it generates the problem

of slow response time. To alleviate this problem, a compensator, which performs feedforward control using torque signals produced by the sliding mode torque observer, is added. The sliding mode state observer offers advantages similar to those of sliding controllers such as robustness to parameter uncertainty, measurement noise and easy application to important classes of nonlinear system [4],[5]. To verify the operating characteristics of the proposed system, the simulation program is developed and the system is implemented by using DSP.

II. FUZZY-SLIDING ADAPTIVE CONTROLLER WITH SLIDING MODE TORQUE OBSERVER

The sliding mode controller have robustness to parameter variations and external disturbance, good tracking response and easy applicability to nonlinear system. To utilize these advantages and reduce chattering, FSAC is developed. To achieve chattering reduction without losing robustness to external disturbance, the sliding mode state observer is added to the fuzzy-sliding adaptive controller. The sliding state observers are considered to be robust to disturbances including measurement noise.

A. Fuzzy sliding adaptive controller

Although the conventional sliding mode controller has high performance characteristics in load and parameter variations, it produces chattering caused by discontinuous inputs. To alleviate this problem the following sliding mode controller can be used. The input U is determined as:

$$U = K_p * |\text{error}| + K_I * \int |\text{error}| dt \quad (1)$$

$$\text{where, } K_p = K_{p1} * \frac{S}{|S| + \delta}$$

$$K_I = K_{I1} * (1 - \frac{S}{|S| + \delta})$$

S is sliding surface,

δ is arbitrary positive constant,

$|\text{error}| = |\text{Command value} - \text{real value}|$

The proportional gain (K_p) and integral gain (K_I) of equation (1) are inferred by using following fuzzy logic.

- if error is large then K_p is large
- if error is small then K_p is small
- if error is large then K_I is small
- if error is small then K_I is large

Fig.1 and fig.2 show membership functions for the gains K_p and K_I

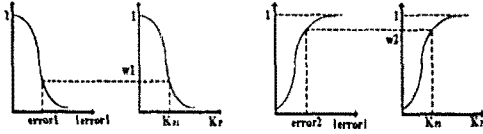


Fig.1. Membership function of proportional gain K_p

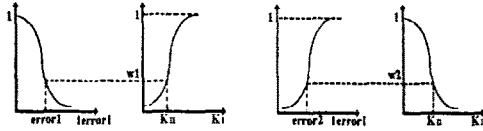


Fig.2. Membership function of integration gain K_I .

Using membership functions, the gains of the FSAC are determined.

$$K_I = \frac{w_1 * K_{I1} + w_2 * K_{I2}}{w_1 + w_2} = \frac{w_1 * f_1^{-1}(w_1) + w_2 * f_2^{-1}(w_2)}{w_1 + w_2} = F(w_1, w_2) = F(\text{error}_1, \text{error}_2) \quad (3)$$

where, $w_1 = \frac{S}{|S| + \delta}$,

$$w_2 = (1 - \frac{S}{|S| + \delta})$$

Finally, gains K_p and K_I are obtained.

$$K_p = (K_{p1} - K_{p2} * e^{-K_{p3}|\text{error}|})$$

$$K_I = K_{I1} * e^{-K_{I2}|\text{error}|} \quad (4)$$

The range of gains K_p and K_I are given as shown in fig.3. Although the gains of the FSAC are changed continuously, they do not produce any stability problem. However the system generates the problem of slow

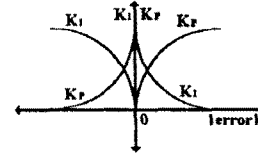


Fig.3. Range of K_p and K_I

response time, although chattering is reduced. To alleviate this problem, a SMTO is designed, then the estimated torque is feedforwarded to the FSAC. Fig.4 shows a block diagram of a FSAC with a SMTO.

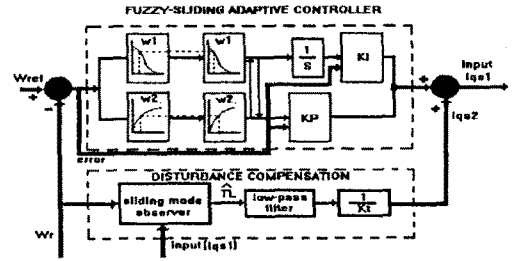


Fig. 4. A block diagram of a FSAC with a SMTO.

B. Design of a sliding mode torque observer

Considering modelling error, measurement noise, and load disturbance, the system can be represented as a linear continuous time-invariance system. The state equation of this system is

$$\frac{d}{dt} \begin{bmatrix} \omega_r \\ T_L \end{bmatrix} = \begin{bmatrix} -B/J & -1/J \\ 0 & 0 \end{bmatrix} \begin{bmatrix} \omega_r \\ T_L \end{bmatrix} + \begin{bmatrix} K_T/J \\ 0 \end{bmatrix} I_{qs} - DW$$

$$\omega_r = [1 \ 0] \begin{bmatrix} \omega_r \\ T_L \end{bmatrix} + \eta_2 \quad (6)$$

where, ω_r = Speed

T_L = Load Torque

I_{qs} = Control input ('q' axis motor current)

$DW = [\eta_1 \ 0]^T$ (modelling error)

η_1 = Modelling error

η_2 = Measurement noise

$K_i = (3P/4)(L_m^2/L_r)i_{ds}^*$

L_m = Mutual inductance

L_r = Rotor inductance

P = Number of poles

i_{ds}^* = Flux current command

J = Mechanical inertia constant

B = Mechanical viscous friction constant

Consequently, the system is observable. If the sliding

mode observer using above represented $\text{sgn}(\cdot)$ function is built, the system is given as follows:

$$\begin{aligned} \hat{\omega}_r = & -\frac{B}{J} \cdot \hat{\omega}_r - \frac{1}{J} \cdot \hat{T}_L + \frac{K_T}{J} \cdot I_{qs} \\ & + K_1 \cdot \text{sgn}(\hat{\omega}_r - \omega_r) \end{aligned} \quad (7)$$

$$\hat{T}_L = K_2 \cdot \text{sgn}(\hat{\omega}_r - \omega_r) \quad (8)$$

where, $\hat{\cdot}$ denotes an estimated value

Fig. 5 shows a block diagram of the sliding mode observer.

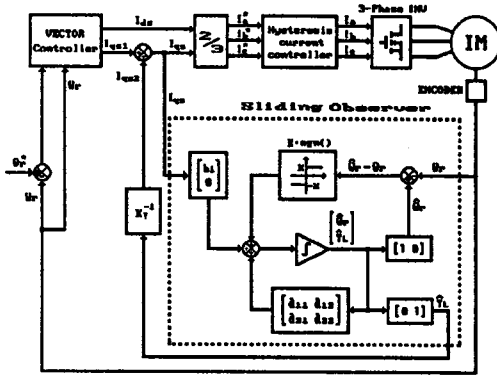


Fig.5. A block diagram of the sliding mode observer.

The sliding mode hyperplane is

$$S = \hat{\omega}_r - \omega_r = 0 \quad (9)$$

To generate sliding mode, the existence condition of sliding mode is

$$S\dot{S} < 0 \quad (10)$$

Then, allowable range of the switching gain K_1 and K_2 are obtained as

$$K_1 < -\Delta_{\max}, \quad K_2 = -LK_1 \quad (11)$$

where, $\Delta_{\max} = \max [(-J/B)\omega_r - \sqrt{s}]$

The discrete-state model of the sliding observer is given as follows:

$$x(k+1) = \Phi x(k) + \Gamma u(k) \quad (12)$$

$$y(k) = Cx(k) \quad (13)$$

where, $\Phi = e^{AT}$, $\Gamma = \left(\int_0^T e^{AS} dS \right) B$
 $T = \text{Sampling Time}$

Transforming (7), (8) into the discrete system, the discrete-state model becomes as follows:

$$\Phi = \begin{bmatrix} a_{11} & a_{12} \\ a_{21} & a_{22} \end{bmatrix} \quad (14)$$

$$\Gamma = [b_1 \ b_2]^T \quad (15)$$

where, $a_{11} = e^{-B \cdot T/J}$,

$$a_{12} = -\left(\frac{P}{2}\right)(1 - e^{-B \cdot T/J})/B$$

$$a_{21} = 0 \quad a_{22} = 1$$

$$b_1 = \left(\frac{P}{2}\right) \cdot (K_T/B) \cdot (1 - e^{-B \cdot T/J})$$

$$b_2 = 0$$

The sliding mode observer output is added into command current feedforwardly.

$$I_{qs2} = \frac{1}{K_T} \cdot \hat{T}_L \quad (16)$$

$$I_{qs} = I_{qs1} + I_{qs2} \quad (17)$$

In servo system, to estimate parameter quickly, the poles of system can be placed at (0,0) in Z-plane. The method is, namely, deadbeat control. The response time of the state observer has to be faster than that of the whole system.

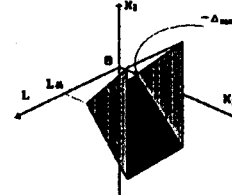


Fig.6. Range of improved sliding observer gains.

To satisfy this condition, the range of improved sliding observer gains K_1 , K_2 and observer pole L are have to be located in the dashed area as shown by fig. 6.

III. SYSTEM CONSTRUCTION AND SIMULATION RESULTS

A block diagram of the indirect vector-controlled induction motor drive system is shown in fig.7. This system consists of an induction motor loaded with a dc generator, a ramp comparison current-controlled PWM voltage source inverter, a field orientation mechanism, a coordinate translator, and a speed control loop. Using reference frame theory and linearization technique, the vector-controlled induction motor drive system can be represented by the system block diagram as shown in fig.7, where $G_c(s)$ is

the proposed speed controller.

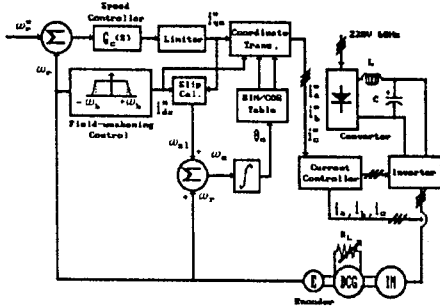


Fig.7. A block diagram of the proposed system.

The digital FSAC is

$$U(z) = K_P' + \frac{K_I'}{1 - z^{-1}} \quad (18)$$

where, $K_P' = (K_{p1} - K_{p2} * e^{-K_{p2}|error|}) * (1 - \frac{T * K_{p1} * e^{-K_{p2}|error|}}{2})$,
 $K_I' = (K_{p1} - K_{p2} * e^{-K_{p2}|error|}) * (K_{p1} * e^{-K_{p2}|error|}) * T$,
 T = Sampling time

Fig.8 shows speed responses of FSAC, PI controller, PI controller with SMT0 and FSAC with SMT0 respectively when 2Khz sampling frequency is used. It can be seen that the fuzzy-sliding adaptive controller has better speed response than that of the PI controller.

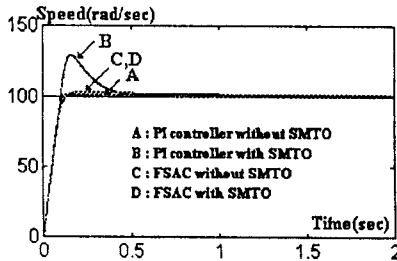
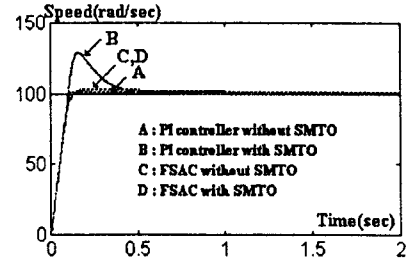


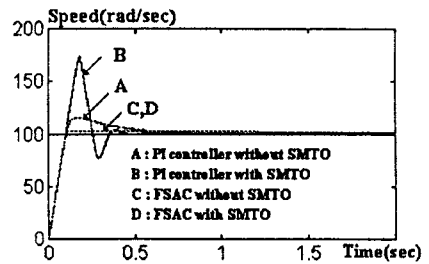
Fig. 8. Dynamic characteristics of FASC, PI controller, PI controller with SMT0 and FSAC with SMT0.

Fig.9 shows speed response of the FSAC and PI controller, PI controller with SMT0 FSAC with SMT0 when sampling frequency is varied. In fig.9 (b),(c), the variations of sampling time means the variations of the parameter and gain. Thus, the speed response of PI controller are affected by sampling frequency. Fig.10 shows the speed responses of PI controller, FSAC, PI

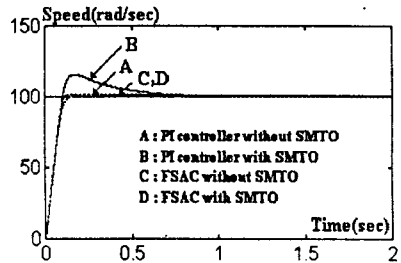
controller with SMT0, and FSAC with SMT0 when the system parameter \hat{J} is changed. It can be seen that from fig.10, even with more than 50% changes, both sliding mode observer and FSAC has adaptive capability to the modelling error.



(a)



(b)



(c)

Fig. 9. Dynamic characteristics of PI controller, FSAC, PI controller with SMT0 and FSAC with SMT0 when sampling frequency is varied with values of (a) 2Khz (b) 10Khz (c) 1Khz).

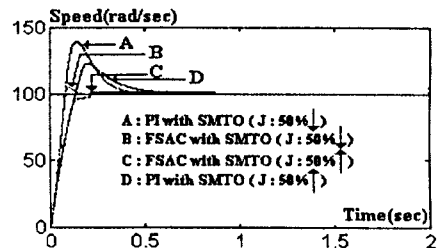


Fig.10. Dynamic characteristics of PI controller, FSAC, PI controller with SMT0 and FSAC with SMT0 when the system parameter \hat{J} is changed.

PI controller with SMT0 and FSAC with SMT0 when the system parameter is changed.

Fig.11 shows the speed responses of PI controller, FSAC, PI controller with SMT0, and FSAC with SMT0 when 120% of the rated load is applied for 1 to 1.5 sec.. In fig.11, 'C' is the speed responses with removal of chattering by using FSAC. 'D' is the speed response when the SMT0 is added to improve the robustness to the load, and the filter is also added to reduce the ripple component of the sliding mode torque observer output.

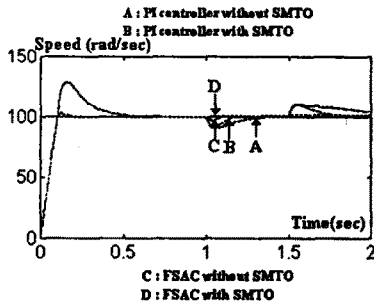


Fig. 11. Dynamic characteristics of PI controller with SMT0, FSAC with SMT0 when the load is applied.

IV. EXPERIMENTAL RESULTS

The designed system was implemented using DSP TMS320C31. Fig.12 shows speed responses of the FSAC and PI controller when 2Khz sampling frequency is used.

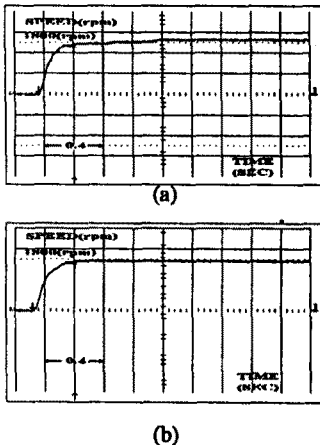
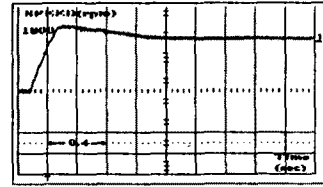


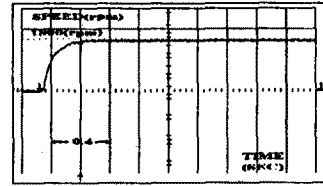
Fig.12, Dynamic characteristics of PI controller and FSAC with (a) PI controller (b) FSAC.

Fig. 13 shows the speed responses when the sampling

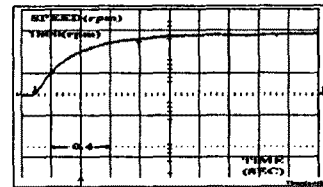
frequency is varied. From fig.13, we can see that the system with FSAC is robust to the variation of sampling



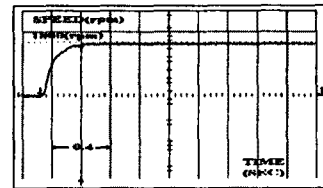
(a)



(b)



(c)

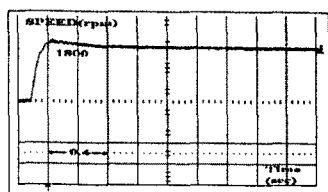


(d)

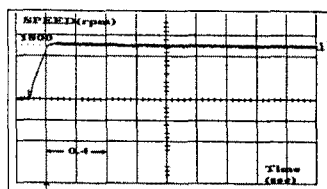
Fig. 13. Dynamic characteristic of PI controller and FSAC when sampling freq. is

- (a) PI controller (sampling freq. =10Khz),
- (b) FSAC (sampling freq. =10Khz),
- (c) PI controller (sampling freq. =1Khz),
- (d) FSAC (sampling freq. =1Khz).

Fig.14 shows the speed responses of FSAC with SMT0 when the value of \hat{J} is decreased by 50% compared to the rated value. As described in simulation results, the FSAC with SMT0 has robustness to the parameter change. Fig.15 shows the speed responses of PI controller, FSAC, PI controller with SMT0 and FSAC with SMT0 when 120% of the rated load is applied for 1 to 1.5 sec.. It can be seen that the FSAC with SMT0 is robust to the load change.



(a)

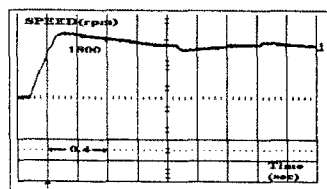


(b)

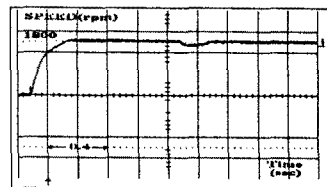
Fig.14. Dynamic characteristics with paramter change

(a) PI controller with SMT0,

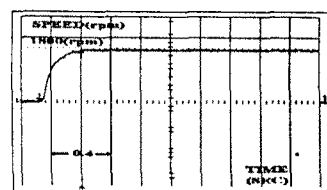
(b) FSAC with SMT0.



(a)



(b)



(c)

Fig. 15. Dynamic characteristics with load torque variations

(a) PI controller with SMT0,

(b) FSAC,

(c) FSAC with SMT0.

V. CONCLUSION

In this paper, a high performance FSAC using SMT0 for an induction motor is proposed. The FSAC removes

the problem of oscillations caused by discontinuous inputs of the sliding mode controller. The controller also provides robust characteristics against parameter and sampling time variations. Although, however, the performance of FSAC is better than PI controller and fuzzy controller in robustness, it generates the problem of slow response time when the load is changed. To alleviate this problem a compensator, which performs feedforward control of the torque signals produced by the SMT0, is added. The simulation and hardware implementation results show that the proposed system is robust to the load disturbance, parameter variations, and measurement noises.

REFERENCES

- [1] B.K.Bose, *Power Electronics and AC Drives*, 1986.
- [2] Y.Dote, *Servo Motor and Motion Control Using Digital Signal Processors*, Prentice Hall and Digital Signal Processing series Texas Instruments, 1990.
- [3] M.H.Park, K.S.Kim and Y.R.Kim, "Chattering reduction in position control of induction motor using the sliding mode", IEEE/PESC'89 Record, 1988, pp.438-445.
- [4] B.D Yoon, Y.H Kim, C.S Kim, C.K Kim, "Robust Speed Control of Induction Motor Using Sliding Mode State Observer", IPEC, JIEE Conf., YOKOHAMA, JAPAN, 1994, pp.87-pp.92.
- [5] Y.Dote, "Stabilization Controlled Current Induction Motor Drive system via New Nonlinear State Observer" IEEE Trans. IECI, 27(2), 77, 1980.
- [6] U.Itkis, *Control System of Variable Structure*, 1976, pp.14-16.
- [7] G.Min Liaw, F.J Lin, "A Robust Speed Controller for Induction Motor Drives", IEEE Tran., Industrial Elec., vol. 41, No.3, 1994, pp.308 - pp.315.
- [8] Paul C. Krause, *Analysis of Electric Machinery*, McGRAWHILL, 1987.
- [9] W. Leonard, *Control of Electrical Drives*, Springer-Verlag, 1985.
- [10] Texas Instrument, *TMS320C3X user's guide*, 1990.
- [11] P.Vas, *Vector Control of AC Machines*, Clarendon Press, 1990.
- [12] F.L. Lewis, *Applied Optimal Control And Estimation*, Prentice Hall and Digital Signal Processing series Texas Instruments, Prentice Hall Inc., 1992.